

EBSD and BKD

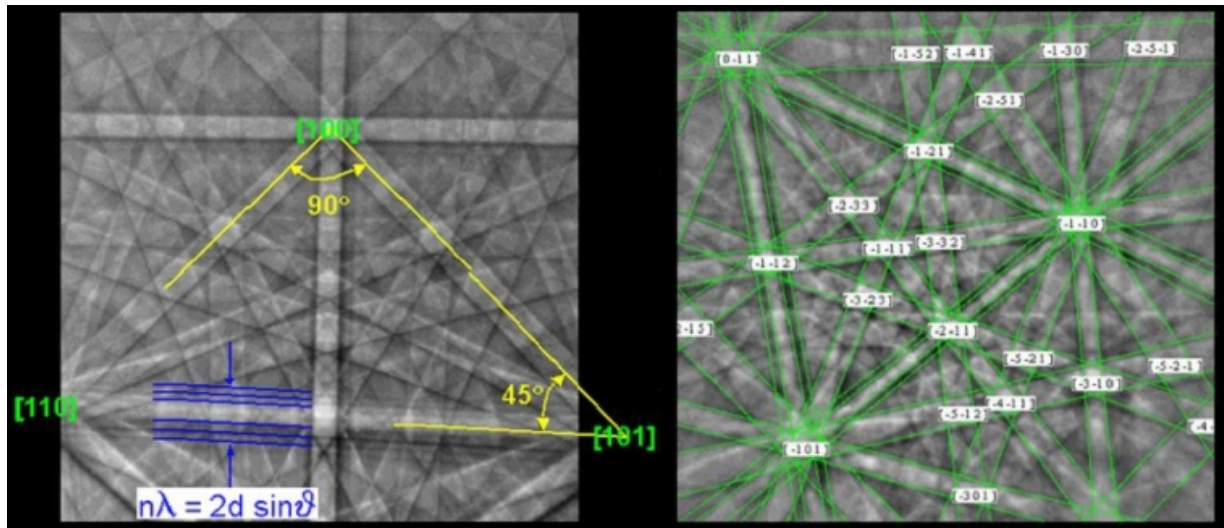
[Home](#)
[Basics](#)
[TKD](#)
[FastEBSD](#)
[Evaluation](#)
[Conclusions](#)
[Publications](#)
[Downloads](#)
[Glossary](#)

Pattern Solving



1. Indexing a Kikuchi Pattern

A Kikuchi pattern can be interpreted as a gnomonic projection of the crystal lattice under the beam spot on the flat registration screen. The angles between the centerlines of bands correspond to interplanar angles of the crystal lattice, and the bandwidths correspond to the reciprocal interplanar distances (pattern on the left). This means that the geometry of a Kikuchi pattern is specific to the structure and the orientation of the crystallite. The most important step in pattern solving is to precisely determine the positions of Kikuchi Bands. Thus, after locating at least three bands, an optimal fit of the lattice planes is sought by checking through the Miller indices allowed by the structure factor of the crystal lattice under consideration. Finally, by simulating the pattern, it is verified that the grain orientation and the chosen crystal structure best fit the pattern. This check can also be illustrated by superposing the theoretical pattern on the experimental one (pattern on the right).



2. Radon versus Hough Transformation

2a. The Radon Transformation

To index a Kikuchi pattern, one only needs to know the positions and widths of some bands. While a skilled user can easily detect even diffuse bands on a strong background, automatic band localization is a task not so easily accomplished with software. It has been proven in practice to locate the bands by applying a Radon transform to the Kikuchi pattern.

The Radon transformation [1] is a continuous function that projects the intensity distribution $f(x, y)$ along a line S in an image into Radon space. The transformation process is defined by the line integral

$$Rf(s) = \int_S f(x, y) ds . \quad (1)$$

In particular, a straight line S can be parametrized as $bx + ay = ab$ (x -intercept y -intercept equation) or

$$\rho_i = x \cdot \cos \varphi_i + y \cdot \sin \varphi_i \quad (2)$$

and thus, the line integral can also be written as

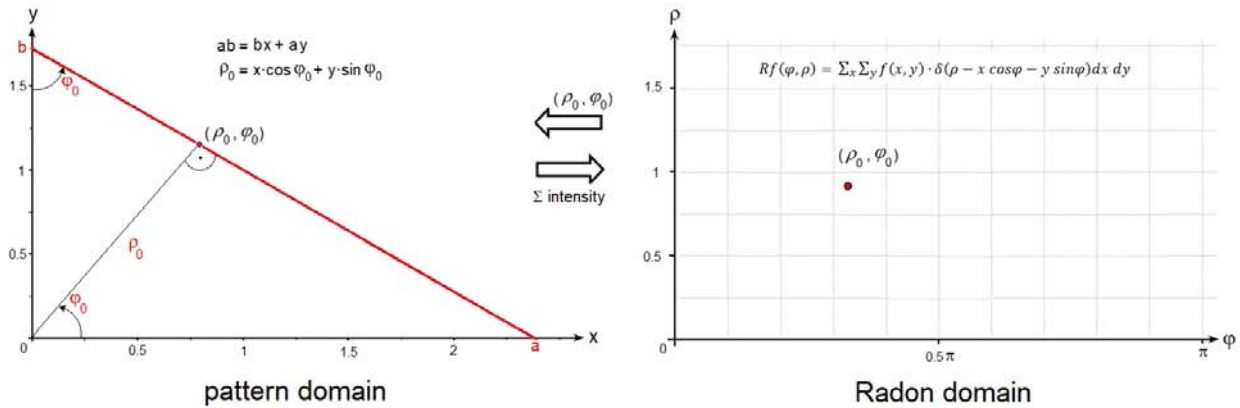
$$Rf(\varphi, \rho) = \iint_{-\infty}^{\infty} f(x, y) \cdot \delta(\rho - x \cos \varphi - y \sin \varphi) dx dy . \quad (3)$$

ρ is the distance of the straight line from the coordinate origin and φ is the angle between the x -axis and the perpendicular to the origin (i.e. the point at the center). φ is limited to $0 \leq \varphi < 2\pi$. δ denotes the Dirac delta function. Thus, a straight line in a 2D

image domain is associated to exactly one point (ρ, φ) in the 2D Radon domain.

A discrete image, here the digitally recorded Kikuchi pattern, consists of a matrix $f[x, y]$ of gray-scale image points called pixels. We must therefore consider a discrete Radon transform, with the integrals in equations 1 and 3 replaced by sums. The image domain and the Radon domain consist of arrays of discrete cells on a Cartesian grid (x, y) and a grid (ρ, φ) , respectively. The sizes of the cells have to be adjusted to the resolution of EBSD measurement. A Kikuchi band can be thought of as a bundle of straight lines slightly rotated and shifted with respect to each other. Thus, using the Radon transform in equation 3, the intensity profile of a band is mapped pixel by pixel not in a sharp point, as would be the case with a single straight line, but smeared out in a kind of "butterfly" motif in the Radon domain.

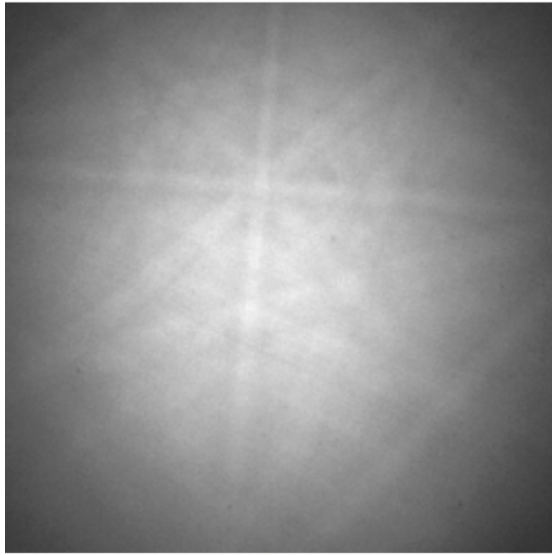
The concept of Radon transformation has some advantages for band localization [2, 3]. A clever approach is to traverse the domain in Radon space inversely cell by cell (ρ, φ) , instead of scanning through the Kikuchi pattern directly and transforming pixel by pixel into the Radon domain. Thus, one first sums up the intensity values along the corresponding straight line, that is the projection line S , in the pattern and then writes this value to the respective cell in one step. Since successive points on the straight line are considered, the intensity profile along the line can be interrogated. For example, sections of the straight line have similar intensity inside a band and a cusp or a peak at the bordering Kikuchi lines. Short sections indicate lines that run (partly) outside a band, and these sections can be skipped during the transformation by applying a run-length filter. Similarly, artifacts and intensity peaks ("hot spots") can be masked out by applying local bounds along the intensity profile. Locally excessive intensity values occur at the zone axes, for example, while diffraction points or dynamic diffraction effects can cause unusually high or low intensity modulations. Applying a nonlinear intensity operator to the domain [3] can further suppress noise and effectively improve contrast. Overall, intensity evaluation along straight lines with the "inverse" construction of the Radon transform results in a clean domain in Radon space.



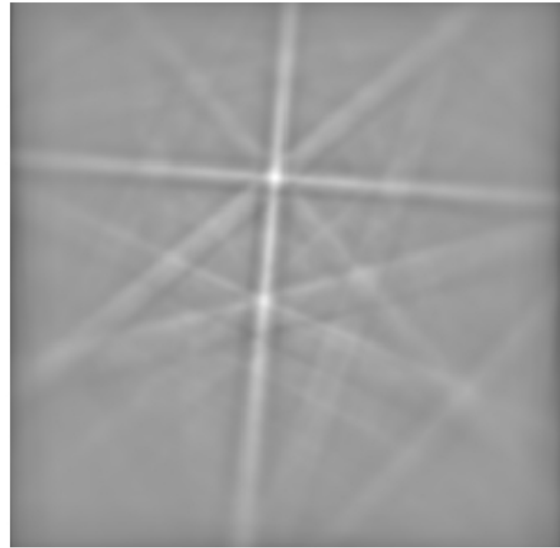
An image similar to the pattern can be reconstructed from its Radon transform using the back-projection operator:

$$Bf(x, y) = \int_0^\pi Rf(\varphi, \rho) d\varphi . \quad (4)$$

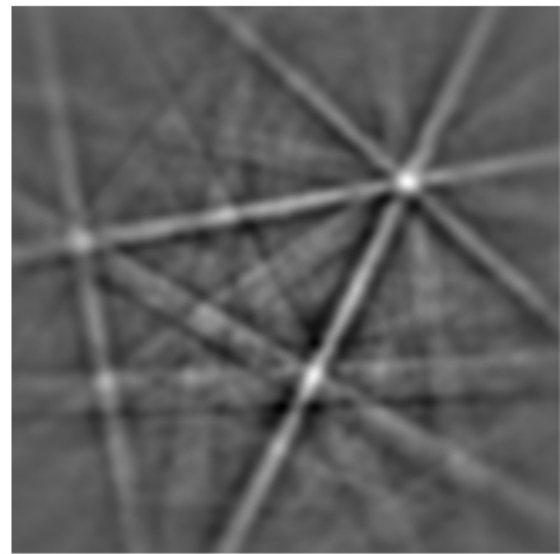
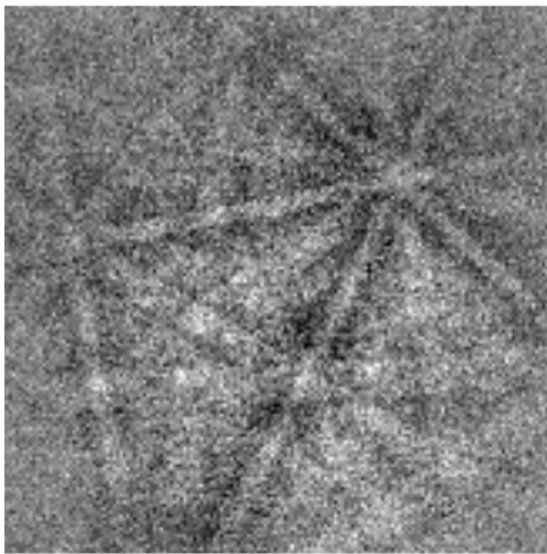
The inverse transform specifies which straight line in the image space is associated with each cell in the Radon domain, and the stored intensity is equally attributed to all points on that line. The Radon backprojection does not provide the original image but produces a smoothed image. In general, statistical noise is reduced. The Kikuchi bands are bordered by slightly hyperbolic instead of straight lines. This may cause a further blur.



Backscatter Kikuchi pattern



From HT backtransformed pattern



Applying a Radon transformation to the Kikuchi pattern simplifies the inherently difficult task of locating lines and bands, since only isolated peaks in the Radon domain need to be found. The "butterfly-like" peaks are best located by a peak search with constraints or by evaluating some coefficients of a 1D FFT of the radon domain along ρ -direction. These peaks are assigned to Kikuchi bands in the pattern according to the inverse Radon transform [3].

2b. The Hough Transformation

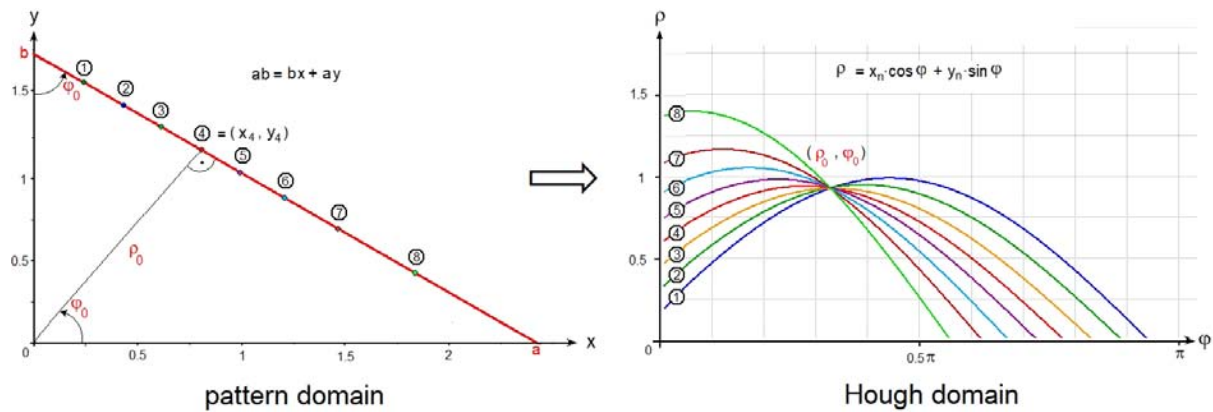
Forty-five years after the publication of the Radon transformation, the Hough transformation was proposed by Paul V.C. Hough in a patent [4]. The underlying objective was to locate straight lines in a discrete image with binary intensity distribution $f_b(x, y)$, which originally represented particle tracks in a bubble chamber in the slope-intercept parametrization $y = b - b/a x$. A modern definition is

$$Hf_b(\varphi, \rho) = \sum_x \sum_y f_b(x, y) \cdot \delta(\rho - x \cos \varphi - y \sin \varphi) dx dy . \quad (5)$$

The image domain and the Hough domain are 2-dimensional spaces with Cartesian coordinates (x, y) and (ρ, φ) , respectively. The common interpretation is that each point (x, y) in the image space is transformed into a sinoidal curve

$$\rho(\varphi) = x \cos \varphi + y \sin \varphi . \quad (6)$$

If points (x, y) in the image lie on a straight line, their sinoidals intersect at a common point and their intensity is accumulated to a peak in the Hough domain.



In a binary image, pixels only take a value of either 1 or 0, so the value on each sinusoid is either 1 or 0. The Hough transform is a particularly fast method to locate sparse straight lines with isolated intensity values = 1, because pixels with intensity values = 0 are skipped during the transformation. Only for pixels with $f_b(x, y) = 1$ the sinusoids are calculated and get intensity = 1. Thus, the height of the Hough peaks is equal to the number of intersecting sinusoids, i.e. the number of non-zero points on the corresponding line in the image. The discretization, inverse transform, and subsequent detection of bands are the same as described above for the Radon transform.

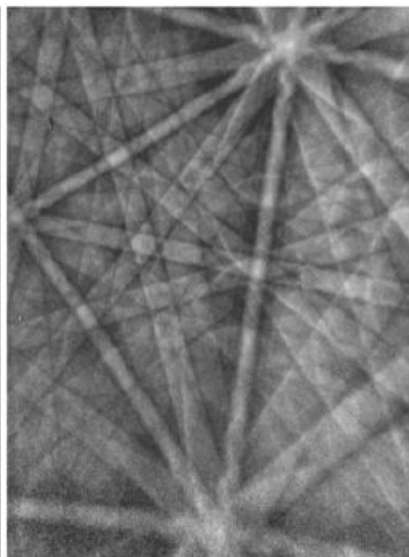
Originally, the discrete Hough transform was defined only for binary (bitonal, 1-pixel) images. In a first step, grayscale images are converted to binary images by an edge filter before the Hough transform is carried out. Since Kikuchi patterns are gray-scale and not binary images, a Hough transform is, strictly speaking, not well suited for band detection. Of course, a gray-scale Kikuchi pattern can be reduced to a binary pattern, and then Hough transformed. The result is a significant loss of information, especially with respect to the band profile used to evaluate a meaningful Pattern Quality (PQ). On the other hand, the speed is increased by about a factor of 1/3, depending on the threshold of binarization (0 or 1) of the intensity levels. Another disadvantage of applying a Hough transform to binary Kikuchi patterns is a lower accuracy of orientation data. A better approach to increase speed, at the expense of accuracy, is to work with a higher binning rate, e.g. 60x60 pixels instead of 100x100 or more pixels per pattern.

The discrete Hough transform was therefore "modified" in [5] to account for and evaluate gray-scale patterns. Thus it loses the advantage of high speed by skipping pixels with zero intensity. The result is quite similar to that of the Radon transformation without the run-length filter. The theory and implementations of Radon and Hough transformations are presented in detail in [6, 7]. The Hough transformation and, moreover, its modification for grayscales are special cases of the Radon transformation. The essential difference between the Radon transform and the "modified" Hough transform in BKP analysis lies in the method of how the transformed domains are constructed from the image domain.

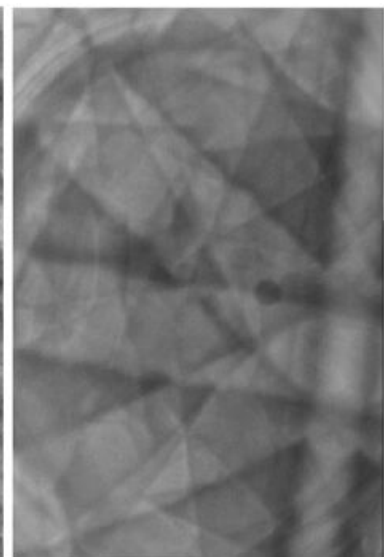
In early EBSD analyses, peaks were located in the "Hough" domain by applying a normalized cross-correlation process with a large "butterfly-shaped" filter mask. In the simplest model, a rectangular pot profile was applied to the band intensity [11]. The main drawbacks of this method are the dependence of the band profile on the position of the band in the Kikuchi pattern, the type of pattern, the diffraction geometry, the accelerating voltage, the grating type, and the $\{h k l\}$ of the band to be detected. To satisfy this, the filter mask must be matched to the current band profile. Incorrectly matched masks will result in inaccurately determined band positions and bandwidths. The wider a band is, the larger the mask would have to be. Large masks increase the computing time extremely. A single mask is generally not sufficient; several masks are required to analyze a pattern. Overall, cross-correlation with a filter mask tends to be ineffective.



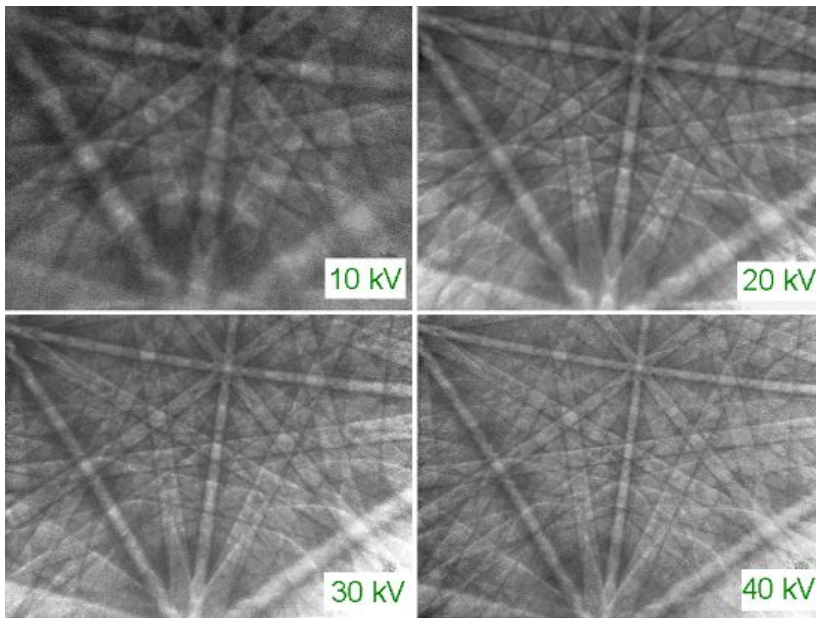
Transmission Kikuchi Pattern
TEM, 250 kV



Backscatter Kikuchi Pattern
SEM, 20 kV



Backsc. Channeling Pattern
SEM, 20 kV



Backscatter Kikuchi Patterns (BKP) of a Nickel Grain

The band profiles and hence the shape of the "butterfly" peaks depend on

- the position of the particular band in the Kikuchi pattern,
- the type of pattern,
- the diffraction geometry,
- the accelerating voltage,
- the crystal lattice and the particular hkl

The conclusion is

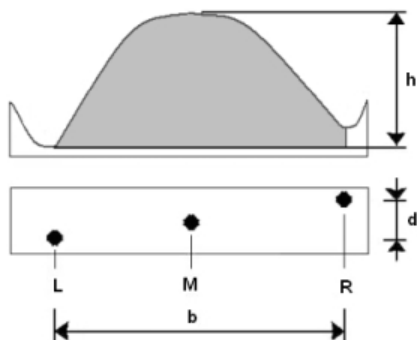
- One mask is not sufficient, several masks are required to analyze one pattern.
- Determination of band positions and band widths is less accurate when using (inadequate) mask(s)
- The wider the bands are, the larger the masks should be. Large masks, however, unduly increase computation time

=> *Cross-correlation with a filter mask tends to be ineffective.*

2c. Conclusion

The Hough formalism obscures the simplicity of the underlying transformation. The designation of Hough transform, however, is prevalent in the EBSD literature, perhaps of not being aware of the origin. The advantages of the Radon transformation include its conceptual simplicity and robustness. S is the path used for integration along the projection lines. For curves that are not straight lines, the natural extension of the Radon transformation is to project along the given curves, e.g., along hyperbolas, which are in fact the exact boundary lines of Kikuchi bands.

3. A simple model of Radon peak profiles illustrates band detection as a constraint task



A simple analysis of Radon peak shapes by measuring the height h , breadth b and displacement d of the cusps L , R and central peak M .

The simplified peak profile model leads to a task with three constraints:

- The cusps L and R are local minima, and M is a local maximum:
 $h \geq h_{\min}$ (peak intensity is above the mean level of intensity.)
 $d \leq d_{\max}$ (skew of the central peak, depends on hkl).
- $b_{\min} \leq b \leq b_{\max}$ (range of Bragg angles ϕ_{hkl} , voltage U , specimen-to-screen distance L , binning)
- The angular distance between neighboring peaks depends on crystal lattice and range of hkl: $\Delta\rho \leq \rho_{\min}$ and $\Delta\Phi \leq \Phi_{\min}$


The constraints are implemented previously as a linked list.

4. Peak verification by Artificial Neural Networks (ANN)

Not all peaks in the Radon space that satisfy the constraints correspond to real bands in a diffraction pattern, since the underlying peak-shape model for band profile analysis is, in the interest of short execution time, as simple as possible and there are artifacts in Radon transforms. To increase the reliability of band extraction, a layered ANN was used to verify the detected bands. ANN are superior to "sharp" verification methods based on numerical comparison of the shapes of actual and theoretical peaks, e.g., by checking a threshold value for the mean square deviation or by a cross-correlation test with a filter mask. The response function of a neuron is "soft" and "fuzzy". It can process a continuous range of intermediate values due to an adjustable sigmoid function. ANN can automatically "learn" complex relationships between data through training. They can be easily adjusted to many different peak profiles that are already present in one pattern, but in particular may vary significantly in general, especially with a change in material or phase, accelerating voltage, or diffraction set-up in general.

A set of three-layer feed-forward neural networks with back-propagation (3L FFwBP) was implemented [2]:

- The number of input neurons, $\#in$, (= pixels on a band profile line) is automatically increased with band width. (The networks range from $10 \times 6 \times 2$ to $20 \times 11 \times 2$ neurons. The number of neurons in the hidden layer is $(\#in + \#out)/2$, the number of output neurons, $\#out$, is two: yes/no.)
- The neural networks were trained by back-propagation on the peak intensity distributions in Radon space of 80 real Kikuchi bands.
- The hit rate exceeds 99.2% of correctly detected bands with 9 bands per pattern.

- [1] J. Radon: Über die Bestimmung von Funktionen durch ihre Integralwerte längs gewisser Mannigfaltigkeiten. Ber. Verh. Sächs. Akad. Wiss. Leipzig, Math.-Naturw. Klasse **69** (1917) 262-267
English translation by P.C. Parks: On the determination of functions from their integral values along certain manifolds. IEEE Trans. Medical Imaging MI-5 (1986) 170-176
- [2] R.A. Schwarzer and J. Sukkau: Automated evaluation of Kikuchi patterns by means of Radon and Fast Fourier Transformations, and verification by an artificial neural network.
Adv. Eng. Mat. **5** (2003) 601-606 (*Download available on request*)
- [3] J. Sukkau and R.A. Schwarzer: Reconstruction of Kikuchi patterns by intensity-enhanced Radon transformation. Pattern Recognition Letters **33** (2012) 739-743 (*Download available on request*)
- [4] Paul V.C. Hough: Method and means for recognizing complex patterns. US Patent 3,069,654 (1962)
- [5] [Download](#)  N. Krieger Lassen: Automated Determination of Crystal Orientations from Electron Backscattering Patterns. PhD Thesis, Technical University of Denmark at Lyngby, 1994
- [6] St. Deans: The Radon Transform and Some of its Applications. John Wiley and Sons, New York 1983. Dover Paperback edition 1993 ISBN 13: 978-486-46241-7
- [7] [Download](#) Peter Toft: "The Radon Transform - Theory and Implementation", Ph.D. thesis. Dept Mathematical Modelling, Technical University of Denmark, 1996

[Home](#)[Basics](#)[TKD](#)[FastEBSD](#)[Evaluation](#)[Conclusions](#)[Publications](#)[Downloads](#)[Glossary](#)